18

Modeling of extinction spectra of silver nanoparticles in colloidal solutions and flexible substrates

© E.A. Ryabov, D.N. Bratashov, E.S. Prikhozhdenko¶

Saratov National Research State University,
410012 Saratov, Russia

¶e-mail: prikhozhdenkoes@sgu.ru

Received December 11, 2023
Revised February 19, 2024
Accepted March 05, 2024

The full realization of the biomedical and technological potential of silver nanoparticles requires reliable methods of their synthesis with precisely controlled size, structure, and morphology. The use of mathematical modeling allows us to obtain a more detailed understanding of the interaction of silver nanoparticles with electromagnetic radiation and determine the optimal parameters to achieve the desired optical properties. This paper presents the results of modeling the effect of silver nanoparticle parameters on extinction spectra in colloidal solutions and on substrates. Calculations were performed in the PyGDM software product based on the dyadic Green method and the volumetric sampling method. The diameter of silver nanoparticles in the simulation of extinction spectra, the positions of the extinction peak were considered in the range 1−85 nm, the refractive indices of the medium varied in the range 1.0−2.4, nonwovens of polycaprolactone ($n = 1.1$) and polyacrylonitrile ($n = 2.4$) were considered as substrates. The simulation was carried out both for single nanoparticles in a colloidal solution and on the surface of a non-woven material, and for a pair of nanoparticles on the surface of a non-woven material with specified gaps between the nanoparticles. In addition to modeling extinction spectra, calculations were carried out for the dependence of the maximum value of the electric field strength caused by laser radiation with a wavelength of 532 nm for silver nanoparticles on a substrate on the gap between particles at different particle diameters (10, 20, 30 nm). It is shown that the resonant extinction peak corresponding to spherical silver nanoparticles increases and shifts towards high wavelengths with increasing diameter. However, the refractive index of the substrate (if any) and the refractive index of the medium have a greater influence on the position of the extinction peak.

Keywords: plasmon resonance nanoparticles, surface-enhanced Raman scattering, extinction spectra, Green's dyadic method, volumetric sampling method.

DOI: 10.61011/EOS.2024.03.58742.28-24

Introduction

Plasmon resonance nanoparticles (NPs) currently find use in such diverse applications as drug delivery [1], deposition of antibacterial coatings [2], and engineering of sensors utilizing surface-enhanced Raman scattering (SERS) [3]. Raman spectroscopy is an analytical method for determination of the structure of molecules based on their vibrational spectra recorded upon inelastic scattering of light [4]. One possible way to enhance the analyte signal intensity is to develop SERS substrates based on plasmon resonance NPs. When two NPs with a small gap interact, a region of locally intensified electromagnetic field, which has the potential to enhance the SERS signal intensity by a factor of 1010 or more and is called a „hot spot" [5], forms between them.

Evaluation of the width of a gap between NPs is an essential part of substrate characterization. At present, nanometer and subnanometer gaps are used for substrates. Transmission electron microscopy (TEM) and scanning probe microscopy (SPM) rank among the current techniques suited for the examination of gaps between NPs. Measurements of such tiny gaps impose strict requirements as to the resolution of instruments and involve highly specific measurement procedures. A simpler approach consists in estimation of the gap size based on the results of theoretical modeling of variation of plasmon absorption spectra with gap width and on experimentally measured extinction spectra. This task has already been worked out quite well [6,7].

The next problem is the study of hot spots produced by closely spaced NPs with the use of flexible substrates, including the experiments on formation of substrates on nonwoven materials consisting of individual fibers [8,9]. A nonwoven material is a polymer matrix consisting of individual fibers. The functionalization of these fibers with silver NPs opened up new opportunities in the field of selective adsorption of biomolecules and their precise detection with the use of SERS [10]. However, it is rather difficult to perform TEM characterization of composite materials of this kind and record extinction spectra in the UV optical region. Calculated data on plasmon absorption spectra of NPs on nonwoven material fibers are virtually lacking in literature.

The results of modeling both for NP suspensions and nonwoven material fibers functionalized with NPs are reported below. Extinction spectra were calculated both for

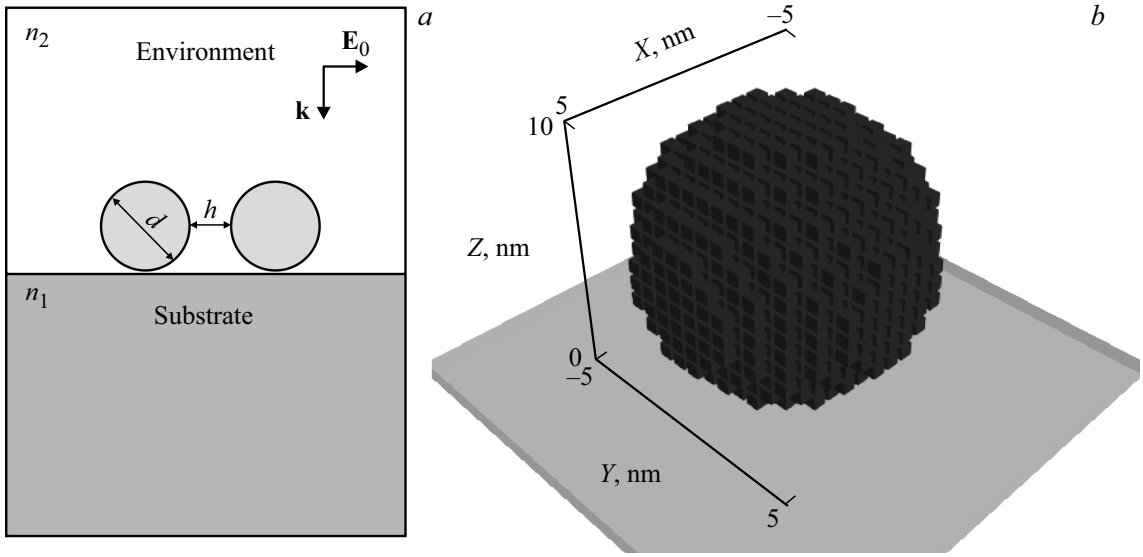

Figure 1. (*a*) Diagram of arrangement of NPs with diameter d and gap h between them in an environment layer with refraction index n_2 on a substrate with refraction index n_1. (*b*) Discretized NP with diameter $d = 10$ nm.

Average value of refraction index n of materials

Material	n
Air	1.0 [14]
Water	1.33 [15]
PCL	1.1 [16]
PAN	2.4 [17]

individual particles as a function of their size and refraction index of the medium and for a pair of particles on the surface of various nonwoven materials.

Model description

The PyGDM software package (an open-source Python toolkit for electrodynamic modeling in nanooptics [11]) was used to measure the optical properties of silver NPs. It operates based on the Green's dyadic method (GDM) and the volumetric discretization method. GDM is an approach to modeling electromagnetic fields that relies on solving Maxwell's equations in the frequency domain with space broken down into finite volumetric elements.

One advantage of GDM over such space discretization methods as FDTD is that only the nanostructure is discretized. For example, a part of the environment around the object of interest needs to be included into the discretization space in FDTD. As a result, the problem may become highly computationally intensive (especially in 3D). Another possible disadvantage of FDTD is the low accuracy of determination of near-field intensities in the case of a dramatic field enhancement (e.g., in plasmonics) [12].

Cubic mesh discretization may be used to model nanostructures of an arbitrary shape made of an arbitrary material.

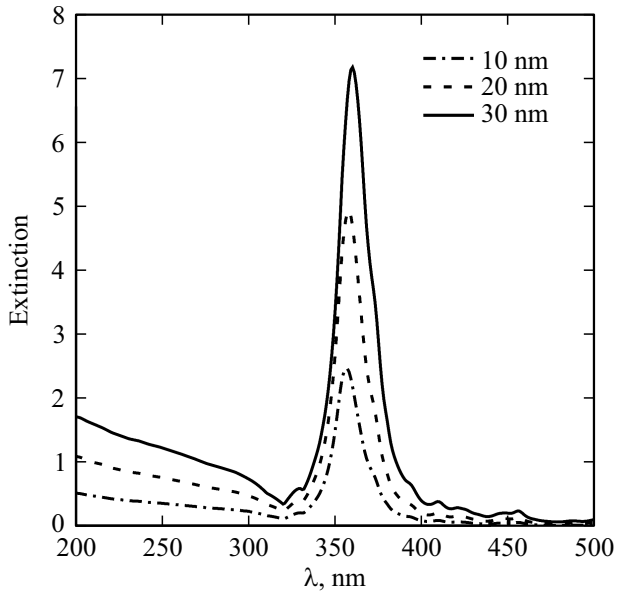

Figure 2. Extinction spectra of silver NPs in solution ($n_1 = n_2 = 1$) for particles of different diameters.

The environment into which a nanostructure is introduced is characterized by dyadic Green's functions used in the calculation. PyGDM implements dyadic Green's functions for a two-layer environment framework (possibly a three-layer framework) with the nanostructure itself positioned in one of the layers. The Lippmann–Schwinger equation, which specifies the electromagnetic field within the entire space, is also used. The electromagnetic field inside the structure (NP) is determined first by solving this equation. In order to determine the electric field outside the structure, the same equation is then used again to repropagate the

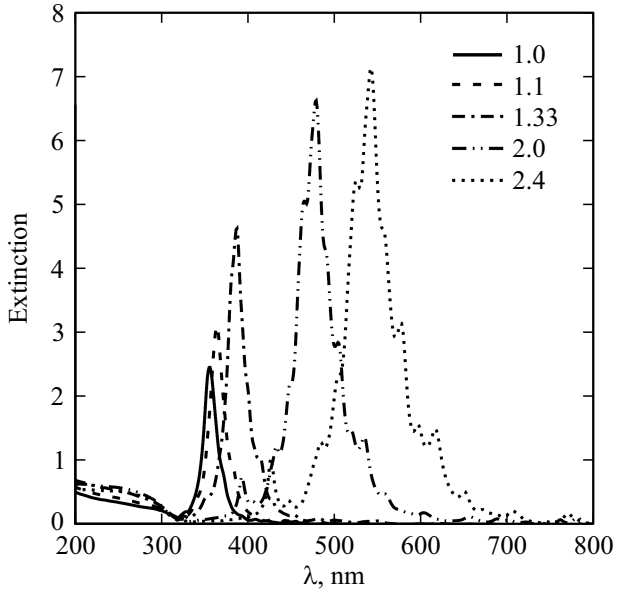

Figure 3. Extinction spectra of silver NPs ($d = 10$ nm) in solution with refraction indices $n_1 = n_2$.

local internal field. To couple layers, one applies either the quasistatic mirror-dipole approximation (if the structures are far away from other layers) or Green's dyads with retardation, which require more computational effort.

The refraction index determined experimentally by Johnson and Christy [13] is used for silver NPs. A description of a substrate with refraction index n1 is produced with the use of Green's tensors. A dielectric medium with refraction index n2 is above the substrate, and silver NPs are located on its surface. The diagram of the modeled structure is presented in Fig. 1 *a*. Figure 1, *b* shows the obtained discretized spherical NP with diameter $d = 10$ nm; this shape is preserved as diameter grows.

Spherical silver NPs are examined in the present study. These NPs form in the process of chemical reduction of silver from ions on the surface of nonwoven material fibers [8,10]. Two substances with different refraction indices were chosen as the substrate material: polycaprolactone (PCL) and polyacrylonitrile (PAN). Air and water (H_2O at a temperature of 25C) were the two considered types of media above the substrate (environment). Although the refraction indices of the above materials depend on wavelength within the 200–800 nm range, the variation is minimal (except for PAN). Therefore, average values of refraction indices [14–16] were used in modeling. The wavelength dependence of the refraction index of PAN within the 300–700 nm range [17] was used to model the corresponding substrate. Refraction indices of substrate materials n_1 and the medium surrounding silver NPs (n_2) are listed in the table [14–17]. It was assumed that $n_1 = n_2$ for NPs in a colloidal solution.

Results and discussion

Modeling an isolated silver NP

Figure 2 shows the diameter dependence of the extinction spectra of silver NPs. The obtained spectra feature extinction peaks within the 360–370 nm range that are characteristic of a colloidal solution of silver NPs. As the NP size increases, the extinction peak shifts to slightly longer wavelengths.

However, the refraction index of the medium in which silver NPs are located exerts a greater influence on the shift and position of their extinction peak (Fig. 3). The extinction peak shifts from 360 to 550 nm as the refraction index of the solution increases from 1 to 2.4. The resulting extinction peaks also broaden in the process. The emergence of peaks is due to volumetric discretization of a spherical silver NP. The emergence of local peaks in the extinction dependences and their growth with increasing refraction index of the medium is due to the NP surface. Similar variations of extinction spectra were observed in [18] for silver NPs with a diameter of 60 nm in an aqueous medium when the roughness of a spherical surface changed.

To gain a deeper understanding of changes in position of the extinction peak of NPs induced by variations of their diameter and the refraction index of the solution, the corresponding dependences were modeled and plotted (Fig. 4). The relative change in position of the NP extinction peak normalized to NPs with a diameter of 1 nm was also calculated (Fig. 4, *b*). The obtained dependences reveal a sharp change in position of the peak occurring when the NP diameter exceeds 30 nm (at refraction indices of the medium $n = 1$ and $n = 1.33$) or 20 nm (at refraction index of the medium $n = 2.4$).

Modeling a pair of silver NPs on a substrate

It is imperative to take the following factors into account when one switches from modeling of colloidal solutions of NPs to functionalized NP substrates based on nonwoven materials: different values of refraction indices of the medium and substrate materials and the influence of the gap width between NPs on the substrate on the resulting electromagnetic field extinction spectra. In order to isolate these factors and examine them separately, an individual silver NP ($d = 10$ nm) on PCL and PAN substrates was modeled first at different values of the refraction index of the medium (Fig. 5). As in the case of colloidal solutions of NPs, an increase in the refraction index of the medium material leads to a noticeable shift and broadening of the NP extinction peak. As the refraction index of the substrate material increases to 2.4, the shift of the extinction peak remains virtually unchanged and similar to the one at $n_1 = 10$; however, this does affect the width and intensity of the extinction peak when the refraction index of the medium increases.

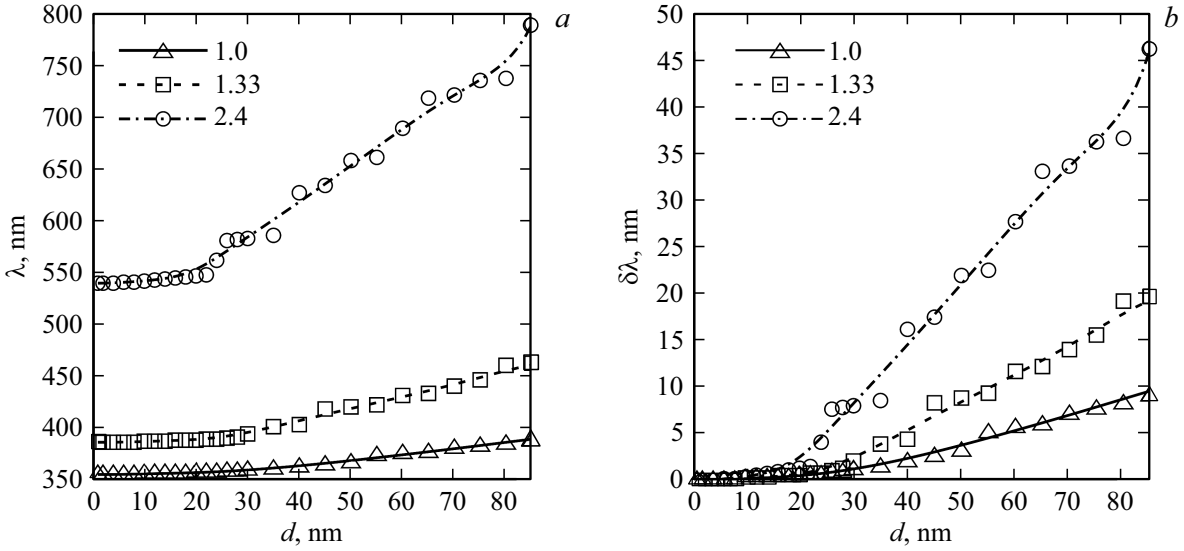

Figure 4. Dependence of the position (a) and the relative change in position (b) of the resonance extinction peak of silver NPs with different diameters in solution at refraction index of the medium $n_1 = n_2$.

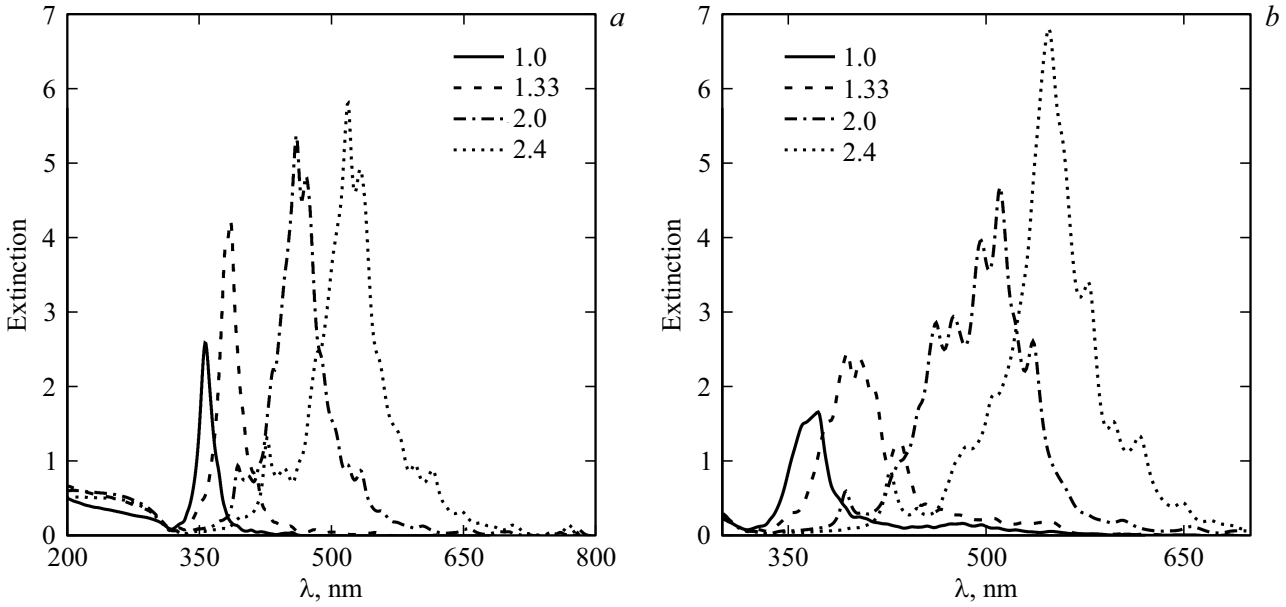

Figure 5. Extinction spectra of silver NPs ($d = 10$ nm) on PCL (a) and PAN (b) substrates at different refraction indices of the medium n_2.

Two silver NPs on the substrate surface with different gaps between them were modeled next. Figures 6 and 7 present the extinction spectra of silver NPs 10 nm in diameter on PCL and PAN substrates, respectively, at gap widths of 0.4–3.4 nm ($n_2 = 1.0$).

Since gaps between NPs on the surface of substrates do not only affect the extinction spectra, but may also be regarded as „hot spots“ for SERS, it is crucial to know how the local electromagnetic field enhancement is distributed. Figure 8 shows the dependences of the maximum electric field strength on the distance between NPs on PCL and PAN substrates, respectively, under laser radiation with wavelength $\lambda = 532$ nm.

It follows from the results of modeling that the maximum electric field strength varies nonlinearly with gap width. This may be attributed to resonance peaks emerging as a result of interaction of vibrating NP dipoles. When the substrate material is switched from PCL to PAN, the shape of extinction spectra changes; as a result, the field strength in the gap between the particles decreases at a wavelength of 532 nm. A more noticeable change is seen in gaps narrower than 1 nm, where the field strength decreases by a factor of approximately 2–3.

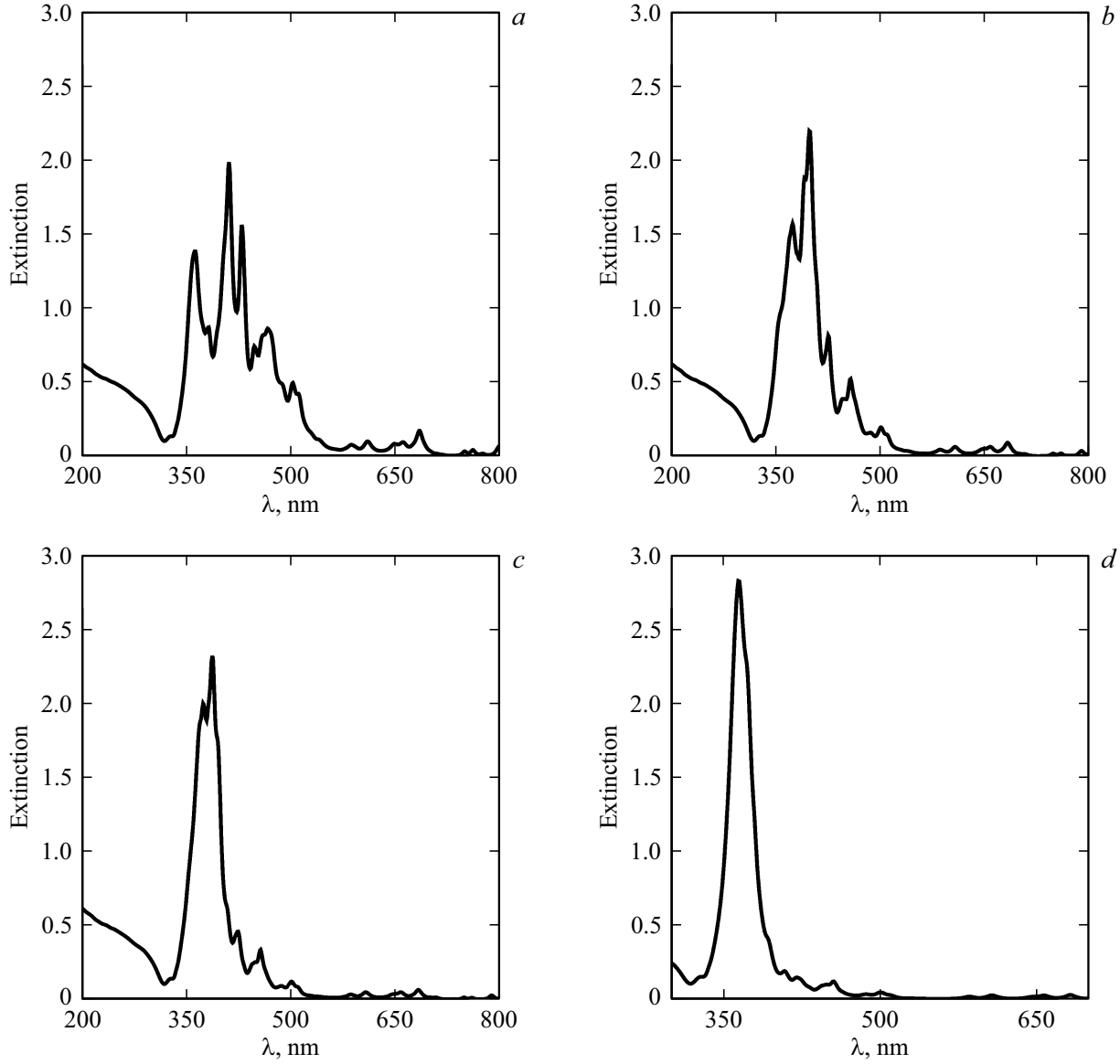

Figure 6. Spectra of the extinction coefficient of silver NPs ($d = 10$ nm) on a PCL substrate at the following widths of gap h between particles: 0.4 (a), 0.8 (b), 1.2 (c), and 3.4 nm (d). The refraction index of the medium is $n_2 = 1.0$.

Conclusion

The influence of particle size and refraction indices of the medium and the substrate on the resulting extinction spectrum of a colloidal solution of silver NPs or silver NPs on the surface of a nonwoven material was examined. The results of mathematical modeling suggest that the refraction index of the medium has a significant effect on the extinction spectra of silver NPs. Specifically, with the refraction index of the medium set to $n = 1.0$ (air) and NPs with a diameter up to 30 nm, the extinction peak shifts insignificantly from 360 nm to 370 nm. When the NP size exceeds 30 nm, the shift becomes more pronounced; at a diameter of 85 nm, the extinction peak is positioned at 395 nm. When the surrounding medium and its refraction index change ($n = 1.33$, water), the extinction peak shifts insignificantly from 390 nm to 400 nm within the range of diameters of silver NPs up to 30 nm. However, as NPs grow in size to 85 nm, the extinction peak shifts more noticeably to 470 nm; measured relative to the peak position for NPs with a diameter of 1 nm, the shift is 20%.

The studied silver NPs had a non-ideal spherical shape: NP surface roughness arose due to cubic mesh discretization. The relation between roughness and NP size was preserved for NPs of all the considered diameters. NP roughness induces the emergence of additional peaks in extinction spectra. Thus, a combination of the refraction index of the medium and the imperfect surface of modeled NPs affects both the position and the profile of plasmon resonance, indicating a complex relation-

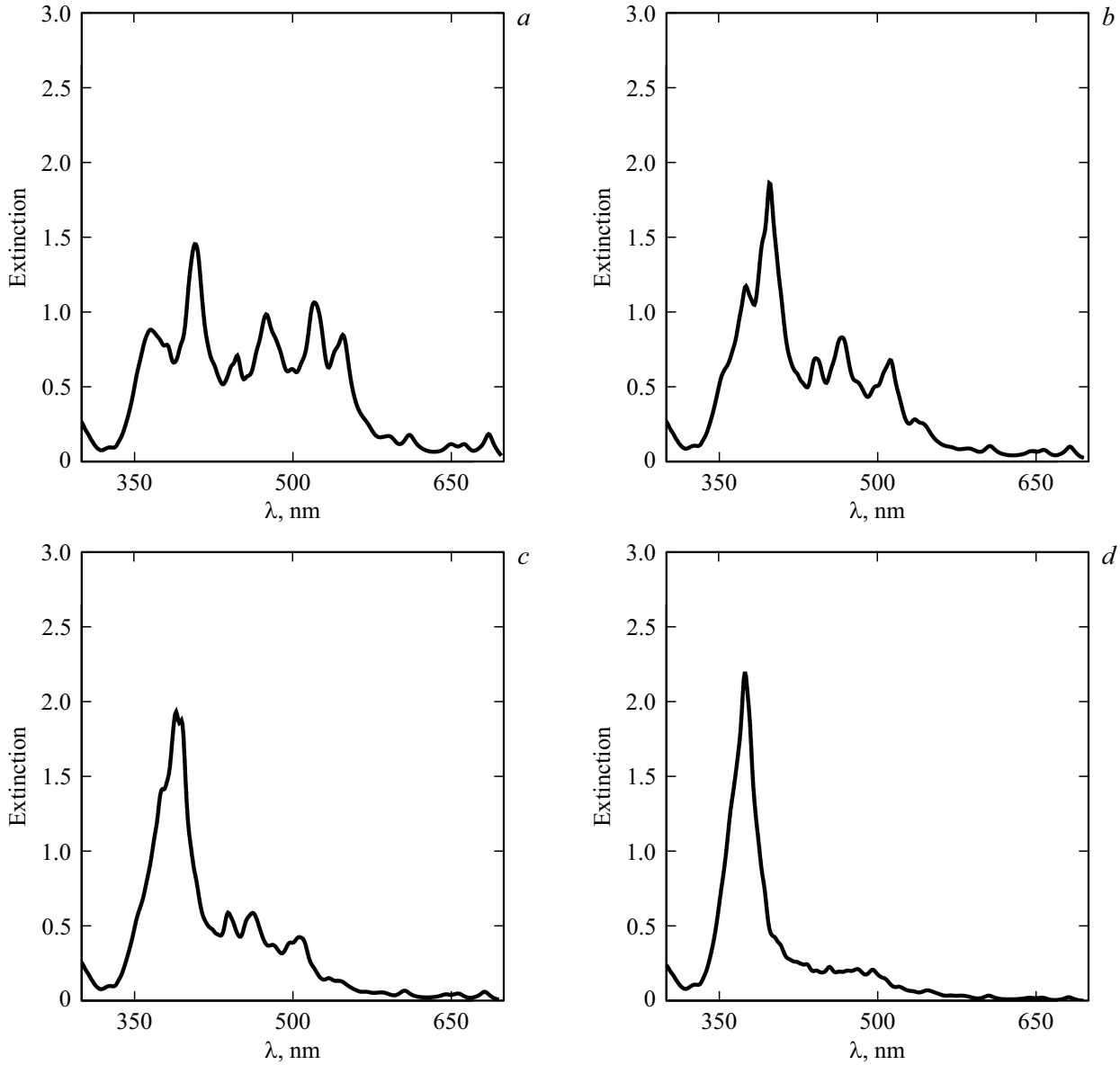

Figure 7. Spectra of the extinction coefficient of silver NPs ($d = 10$ nm) on a PAN substrate at the following widths of gap h between particles: 0.4 (a), 0.8 (b), 1.2 (c), and 3.4 nm (d). The refraction index of the medium is $n_2 = 1.0$.

ship between the optical properties of the surrounding medium and the interaction with NPs located on the substrate.

The width of the gap between a pair of modeled silver NPs on the surface of a substrate affects not only the position of the extinction peak, but also the profile of the resulting extinction spectrum. At gap widths exceeding 1 nm, the observed extinction spectrum profile was similar to the one of an individual silver NP on the substrate.

In addition to modeling the extinction spectra, modeling of the local enhancement of the electromagnetic field was carried out for such substrates. The maximum strength of the field of silver NPs corresponded to PCL substrates, an NP diameter of 30 nm, and an interparticle gap width of 0.5 nm.

Funding

This study was supported financially by the Russian Science Foundation (grant No. 22-79-10270).

Conflict of interest

The authors declare that they have no conflict of interest.

References

[1] J.K. Patra, G. Das, L.F. Fraceto, E.V.R. Campos, M.P. Rodriguez-Torres, L.S. Acosta-Torres, L.A. Diaz-Torres, R. Grillo, M.K. Swamy, S. Sharma, S. Habtemariam, H. Shin. J. Nanobiotechnology, **16** (1), 1–33 (2018). DOI: 10.1186/s12951-018-0392-8

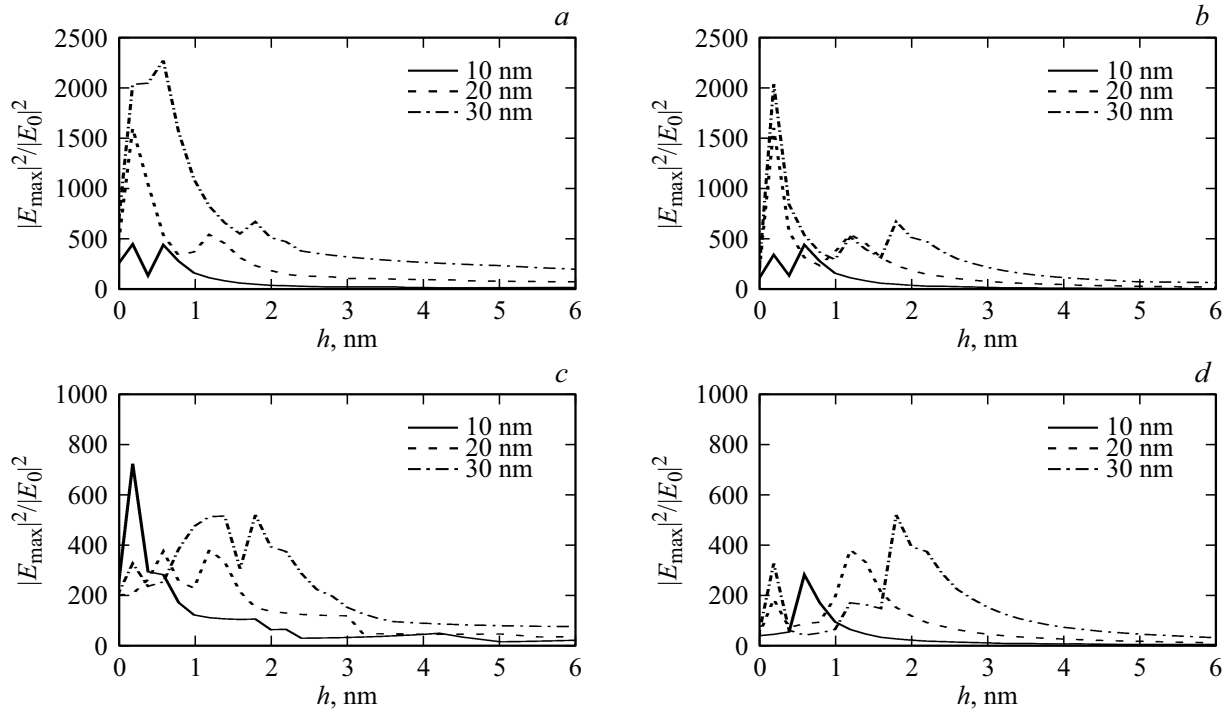

Figure 8. Dependences of the maximum electric field strength of silver NPs on PCL (*a*) and PAN (*c*) substrates on the width of the gap between particles at different particle diameters. Dependences of the maximum electric field strength in the gap between silver NPs on PCL (*b*) and PAN (*d*) substrates on the width of this gap at different particle diameters. The refraction index of the medium is $n_2 = 1.0$. The laser radiation wavelength is 532 nm.

[2] T. Bruna F., Maldonado-Bravo, P. Jara, N. Caro. Intern. J. Molecular Sciences, **22** (13), 7202 (2021). DOI: 10.3390/ijms22137202
[3] T. Dey. Nanotechnology for Environmental Engineering, **8** (1), 41–48 (2023). DOI: 10.1007/s41204-022-00223-7
[4] S. Dawadi, S. Katuwal, A. Gupta, U. Lamichhane,R. Thapa, S. Jaisi, G. Lamichhane, D.P. Bhattarai, N. Parajuli. J. Nanomaterials, 2021, 1–23 (2021).
[5] M. Jiang, Z Wang., J. Zhang. Optical Materials Express, **12** (3),1010–1018 (2022). DOI: 10.1364/OME.451734
[6] N.G. Khlebtsov. Phys. Chem. Chem. Phys., **23** (40), 23141–23157 (2021). DOI: 10.1039/D1CP03057D
[7] B.N. Khlebtsov, A.M. Burov, S.V. Zarkov, N.G. Khlebtsov. Phys. Chem. Chem. Phys., **25**, 30903–30913 (2023). DOI: 10.1039/D3CP04541B
[8] E.S. Prikhozhdenko, D.N. Bratashov, D.A. Gorin., A.M. Yashchenok. Nano Research, **11**, 4468–4488 (2018). DOI: 10.1007/s12274-018-2064-2
[9] G. Liu, Z. Mu, J. Guo, K. Shan, X. Shang, J. Yu, X. Liang. Frontiers in Chem., **10**, 1060322 (2022). DOI: 10.3389/fchem.2022.1060322
[10] M. Saveleva, E. Prikhozhdenko., D. Gorin, A. G. Skirtach, A. Yashchenok, B. Parakhonskiy. Frontiers in Chem., **7**, 888 (2020). DOI: 10.3389/fchem.2019.00888
[11] P.R. Wiecha, C. Majorel, A. Arbouet, A. Patoux, Y. Brûlé, G. Colas des Francs, C. Girard. Computer Phys. Commun., **270**, 108142 (2022). DOI: 10.1016/j.cpc.2021.108142
[12] J. Hoffmann, C. Hafner, P. Leidenberger, J. Hesselbarth, S. Burger. Modeling Aspects in Optical Metrology II, **7390**, 174–184 (2009). DOI: 10.1117/12.828036
[13] P.B.Johnson, R.W.Christy. Phys. Rev. B, **6**, 4370 (1972). DOI: 10.1103/PhysRevB.6.4370
[14] P.E. Ciddor. Appl. Optics, **35** (9), 1566–1573 (1996). DOI:10.1364/AO.35.001566
[15] G.M. Hale, M.R. Querry. Appl. Optics, **12** (3), 555–563 (1973). DOI:10.1364/AO.12.000555
[16] F. Chen, L. Xu, Y. Tian, A. Caratenuto, X. Liu, Y. Zheng. ACS Appl. Nano Materials, **4** (5), 5230–5239 (2021). DOI:10.1021/acsanm.1c00623
[17] M.A. Athal, W.S. Hanoosh, A.Q. Abdullah. Basrah J. Science, **38** (1), 111–130 (2020).
[18] J. Grand, B. Auguié, E.C. Le Ru. Analytical Chem., **91** (22), 14639–14648 (2019). DOI: 10.1021/acs.analchem.9b03798

Translated by D.Safin